Magn Reson Med Sci 2020; 19; 40–47
doi:10.2463/mrms.mp.2018-0124
Published Online: March 26, 2019

MAJOR PAPER

Analysis of Diffusion-weighted MR Images Based on a Gamma Distribution Model to Differentiate Prostate Cancers with Different Gleason Score

Hiroko Tomita[1], Shigeyoshi Soga[1], Yohsuke Suyama[1], Keiichi Ito[2], Tomohiko Asano[2], and Hiroshi Shinmoto[1*]

Purpose: Prostate cancer management includes identification of clinically significant cancers that may require curative treatment. Statistical models based on gamma distribution can describe diffusion signal decay curves of prostate cancer. The purpose of this study was to evaluate the ability of parameters obtained with the gamma model in differentiating prostate cancers with different Gleason score values.

Methods: This study included 155 patients with prostate cancer who underwent multiparametric magnetic resonance imaging prior to prostate biopsy (127 patients) or radical prostatectomy (28 patients) between January 2015 and June 2017; 159 foci of prostate cancer were included in our study. We compared cases scored as Gleason score (GS) 3 + 3 and GS ≥ 3 + 4, and analyzed cases scored as GS ≤ 3+ 4 and GS ≥ 4 + 3 based on the gamma model (Frac < 1.0, Frac < 0.8, Frac < 0.5, Frac < 0.3, and Frac > 3.0), and apparent diffusion coefficient (ADC).

Results: Among 159 cancerous lesions in 155 patients, 13 (8.2%) were GS 3 + 3 prostate cancers, 51 (32.0%) were GS 3 + 4 prostate cancers, 30 (18.2%) were GS 4 + 3 cancers, and 65 (40.9%) were GS ≥ 4 + 4 cancers. Frac < 0.3, Frac < 0.5, Frac < 0.8, and Frac < 1.0 were significantly higher and ADC values were significantly lower in GS ≥ 4 + 3 cancers than in GS ≤ 3 + 4 cancers ($P < 0.01$, $P < 0.01$, $P < 0.01$, $P = 0.01$, and $P < 0.01$, respectively). With receiver operating characteristic (ROC) analysis, Frac < 0.3 and Frac < 0.5 had significantly greater area under the ROC curve for discriminating GS ≥ 4 + 3 cancers from GS ≤ 3 + 4 cancers than ADC ($P = 0.03$, $P < 0.01$, respectively).

Conclusion: Frac < 0.3 and Frac < 0.5 showed higher diagnostic performance than ADC for differentiating GS ≥ 4 + 3 from GS ≤ 3 + 4 cancers. The gamma model may add additional value in discrimination of tumor grades.

Keywords: *apparent diffusion coefficient, gamma model, Gleason score, magnetic resonance imaging, prostate cancer*

Introduction

Prostate cancer is the second-most common cancer diagnosed worldwide and the fifth-most common cancer-related cause of death among men.[1] This condition is diagnosed by measurement of serum prostate-specific antigen levels, digital examination, and transrectal ultrasound-guided prostate biopsy. At present, the major issues in prostate cancer management are related in avoiding unnecessary biopsies and finding clinically significant cancers that may require curative treatment.[2]

Multiparametric magnetic resonance imaging (MP-MRI) is useful for tumor detection, assessment of tumor aggressiveness, and diagnosis of local extension of prostate cancer.[3–6] According to the revised Prostate Imaging Reporting and Data System (PI-RADS version 2),[7] which provides guidelines for interpretation and reporting of MP-MRI results, scores obtained using diffusion-weighted imaging (DWI) and the apparent diffusion coefficient (ADC) map are the dominant parameters for determining the overall PI-RADS score for clinically significant cancer in the peripheral zone.[7] The ADC, which is a metric of DWI, is thought to

[1]Department of Radiology, National Defense Medical College, 3-2 Namiki, Tokorozawa, Saitama 359-0042, Japan
[2]Department of Urology, National Defense Medical College, Saitama, Japan
*Corresponding author, Phone: +81-42-995-1689, Fax: +81-42-996-5214, E-mail: hshinmo@ndmc.ac.jp

Received: September 27, 2018 | Accepted: February 6, 2019

help differentiate between clinically insignificant prostate cancer (Gleason score [GS] = 6) and clinically significant prostate cancer (GS ≥ 7).[7] However, there is considerable overlap in ADCs between clinically insignificant and significant prostate cancer.[8] Thus, further research to identify additional diffusion metrics is warranted to improve the clinical performance of diffusion measurements. In addition, recently, Epstein et al. conducted a large cohort study to verify whether a new grading system, which was approved at the consensus meeting of the 2014 International Society of Urological Pathology and included Grade 1 (GS ≤ 6), Grade 2 (GS 3 + 4 = 7), Grade 3 (GS 4 + 3 = 7), Grade 4 (GS 8), and Grade 5 (GS 9–10), accurately uses a smaller number of grades with the most significant prognostic differences.[9] In their study, they found large differences in recurrence rates between GS ≥ 4 + 3 and GS ≤ 3 + 4 cancers, with 5-year biochemical recurrence-free progression probabilities of 63% and 88%, respectively. Thus, discriminating GS ≥ 4 + 3 from GS ≤ 3 + 4 prostate cancers on the basis of diffusion metrics might be of clinical importance.[10]

The monoexponential model presents ADC values under the assumption that water molecules diffuse freely. However, this approach inadequately describes the complete diffusion process in heterogeneous biological tissues with diffusion-restrictive barriers. Thus, several approaches have been proposed to characterize the non-monoexponential diffusion behavior. In recent years, statistical models based on gamma distribution, which is one of the non-monoexponential models, have proven suitable for describing the diffusion signal decay curves of prostate cancer.[11,12] The gamma model presumes a continuous distribution of diffusion coefficients within the imaging voxel, and the histological interpretation of diffusion data seemed possible by introducing the concept of area fractions for diffusion coefficients $D < 1.0 \times 10^{-3}$ mm^2/s and $D > 3.0 \times 10^{-3}$ mm^2/s as parameters that represent restricted diffusion and perfusion, respectively.[11,12] The purpose of this study was to evaluate the ability of parameters obtained with the gamma model in differentiating prostate cancer with different GS values.

Materials and Methods

Patients

Our Institutional Review Board approved this retrospective study and deemed that patient informed consent was not required. Between January 2015 and June 2017, a total of 168 consecutive patients with pathologically proven prostate cancer had undergone MP-MRI prior to systematic prostate biopsy or radical prostatectomy at our hospital. Of these, 11 patients were excluded because prostate cancer could not be detected on MP-MRI. In addition, two patients were excluded because of severe distortion of the images. Thus, the final study population was composed of 155 patients. Prostate cancer was proven in 127 patients with systematic 12-core transrectal ultrasound (TRUS)-guided biopsies with 2–4 additional targeted biopsies and in 28 patients with radical prostatectomy. Additional targeted biopsies were performed in 23 patients in a cognitive manner. Pathological diagnosis was performed according to the Gleason grading system[13] by board-certified pathologists in our hospital. A summary of the 155 patient characteristics is provided in Table 1.

MR imaging

All examinations were performed on a 3T or 1.5T MR scanner (Achieva 3T and Ingenia 1.5T; Philips Healthcare, Eindhoven, The Netherlands) using a 32-channel phased-array coil. To prevent artifacts from bowel peristalsis, 1 mg of intramuscular glucagon (Glucagon G Novo; Eisai, Tokyo, Japan) was administered immediately before the MRI examination. We used the following hospital prostate imaging protocols: axial and coronal T_2-weighted imaging (T_2WI) (TR/TE = 3500–4000 ms/70–100 ms; section thickness/intersection gap = 3 mm/0 mm; FOV = 160 × 160 mm^2; matrix = 512 × 260, zero-filled interpolation [ZIP] = 1024), DWI (TR/TE = 4000–6500/55–74 ms; section thickness/intersection gap = 3 mm/0 mm; FOV = 240 × 240 mm^2; matrix = 256 × 256; diffusion sensitization gradients oriented along three orthogonal directions at five *b*-values [0, 500, 1000, 1500, and 2000 s/mm^2]), and gadolinium-enhanced dynamic MRI (enhanced T_1-weighted high-resolution isotropic volume

Table 1 A summary of the characteristics of the 155 patients analyzed

Variable	Value
Clinical characteristics	
Age (years)	71.6 ± 7.23* (53–91)
PSA (ng/ml)	11.73† (3.05–11608)
Tumor size (mm)	18.17 ± 10.46*
Surgery	
Systematic prostate biopsy	127
Radical prostatectomy	28
Clinical T stage‡ (%)	
cT_2a	57 (36.8)
cT_2b	4 (2.6)
cT_2c	30 (19.4)
cT_3a	37 (23.9)
cT_3b	19 (12.3)
cT_4	8 (5.2)
Gleason grade§ (%)	
GS 3 + 3	13 (8.2)
GS 3 + 4	51 (32.0)
GS 4 + 3	29 (18.2)
GS 4 + 4 or over	66 (41.5)

*Plus–minus values are means standard deviation; †Median; ‡Number of patients (percentage in total); §Number of lesions (percentage in total); PSA, prostate-specific antigen.

excitation) (TR/TE = 3.8/1.9 ms; flip angle = 15°; section thickness = 3.0 mm [ZIP, 1.5 mm]; FOV = 240 × 240 mm^2; matrix = 240 × 194 [ZIP, 512]). In the dynamic studies, images were sequentially obtained at baseline (unenhanced) and at 25, 60, and 180 s after a bolus injection of 0.1 mmol/kg of gadodiamide hydrate (Omniscan; Daiichi Sankyo, Tokyo, Japan) or gadobutrol (Gadovist; Bayer Pharmaceuticals, Osaka, Japan).

Image analysis

All MR images were transferred to a picture archiving and communication system workstation (EV Insite; PSP corporation, Tokyo, Japan) and were interpreted by two experienced radiologists (H.T., with 5 years of experience in prostate MR imaging and H.S., with 14 years of experience in prostate MR imaging) who were blinded to the patients' clinical history, data, and the histopathological results. For each case, the two radiologists separately assigned PI-RADS scores. In case of disagreement, agreement was reached by consensus. In this study, lesions with PI-RADS scores of 4 or 5, where biopsies or pathologic maps revealed the existence of cancerous tissues, were considered positive for prostate cancer. A suspected cancerous lesion in MRI was considered to be a "positive match" with histologic findings when the tumor was present in the same area of the gland in the pathology report of the TRUS-guided biopsy (Fig. 1). If the standard of reference was radical prostatectomy, MR imaging findings were compared with the whole-mount pathologic specimen where cancer foci were outlined in ink. When the standard of reference was radical prostatectomy, patients were considered to be showing multiple cancerous lesions if the lesions showed distinctly different origins. Finally, 159 foci of prostate cancer were included in our study.

In all cases, the ROIs for prostate cancer were placed on b = 1500 s/mm^2, and measurements were taken by copy–pasting them onto other b-value images (Fig. 1). The ROIs were chosen to be as large as possible, while maintaining minimal contamination from benign prostatic tissues. The measured signal intensities vs. b-value curves were fitted to the gamma model using in-house software. The statistical model based on the gamma distribution has been described in detail elsewhere.[11,12] The parameters of the gamma model adopted in this study include the area fraction of D < 1.0 mm^2/s (Frac < 1.0), D < 0.8 mm^2/s (Frac < 0.8), D < 0.5 mm^2/s (Frac < 0.5), D < 0.3 mm^2/s (Frac < 0.3), and D > 3.0 mm^2/s (Frac > 3.0). The standard ADC value was also calculated using a conventional monoexponential fit with b = 0 and 1000 s/mm^2.

In this report, in addition to comparing cases scored as GS 3 + 3 and GS ≥ 3 + 4, we analyzed cases scored as GS ≤ 3 + 4 and GS ≥ 4 + 3 in terms of the parameters obtained from the gamma model and ADC. Statistical analysis was performed using the Mann–Whitney U test, receiver operating characteristic (ROC) analysis, and Spearman rank-order correlation. For the ROC analyses, the DeLong test was used to compare measures in terms of area under the ROC curve (AUC). MedCalc software suite (version 11.6.2, MedCalc Software; Ostend, Belgium) was used for statistical calculations. P-values <0.05 were considered to indicate a significant difference.

Results

Among the 159 cancerous lesions in the 155 patients, 13 (8.2%) were GS 3 + 3 prostate cancers, 51 (32.0%) were GS 3 + 4 prostate cancers, 30 (18.2%) were GS 4 + 3 cancers, and 65 (40.9%) were GS ≥ 4 + 4 cancers.

Table 2 shows a summary of the statistical results for the gamma model parameters and ADC to differentiate GS ≥ 4 + 3 cancers from GS ≤ 3 + 4 cancers, and GS ≥ 3 + 4 cancers from GS = 3 + 3 cancers. Frac < 0.3, Frac < 0.5, Frac < 0.8, and

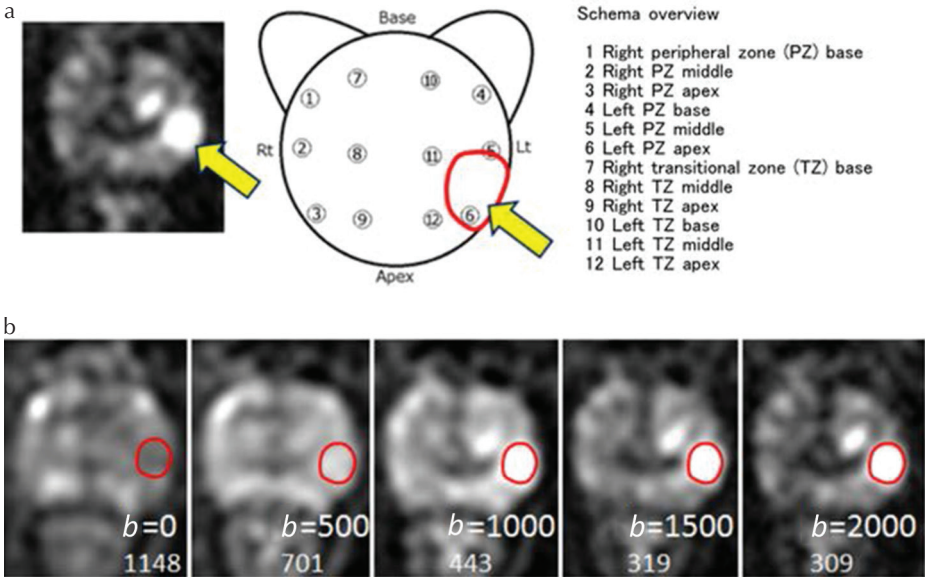

Fig. 1 (**a**) This figure showed target lesions and schema of transrectal ultrasound-guided prostate biopsy. In this biopsy case, prostate cancer was found in 5 and 6 areas of left peripheral zone, and the ROIs was set here (arrows). We set as large as possible ROI for the area where the lesion of prostate cancer was pointed out. (**b**) The ROIs for prostate cancer were placed on b = 1500 s/mm^2, and measurements were taken by copy–pasting them onto other b-value images.

Table 2 A summary of the statistical results for the gamma model parameters and ADC obtained from 159 prostate cancers to differentiate GS ≥ 4 + 3 cancers from GS ≤ 3 + 4 cancers (**a**), and GS ≥ 3 + 4 cancers from GS = 3 + 3 cancers (**b**)

(a)			
Parameter	GS ≤ 3 + 4 (n = 64)	GS ≥ 4 + 3 (n = 95)	P-values
Frac < 0.3 (%)	15.9 ± 6.9	21.9 ± 7.3	<0.01*
Frac < 0.5 (%)	28.9 ± 8.8	31.9 ± 9.0	<0.01*
Frac < 0.8 (%)	45.8 ± 12.0	51.8 ± 11.5	<0.01*
Frac < 1.0 (%)	54.9 ± 13.4	60.0 ± 12.1	0.01*
Frac > 3.0 (%)	9.28 ± 7.5	8.4 ± 6.3	0.59
ADC (mm^2/s)	0.82 ± 0.18	0.72 ± 0.16	<0.01*
(b)			
Parameter	GS = 3 + 3 (n = 13)	GS ≥ 3 + 4 (n = 146)	P-values
Frac < 0.3 (%)	14.0 ± 5.9	20.0 ± 7.7	<0.01*
Frac < 0.5 (%)	26.6 ± 7.0	33.6 ± 9.6	<0.01*
Frac < 0.8 (%)	43.9 ± 12.1	49.9 ± 12.0	0.04*
Frac < 1.0 (%)	52.9 ± 13.7	58.4 ± 12.7	0.07
Frac > 3.0 (%)	10.2 ± 7.2	8.6 ± 6.8	0.46
ADC (mm^2/s)	0.86 ± 0.17	0.75 ± 0.17	0.03*

*Significant (P < 0.05); Mean ± standard deviation; P-values indicate the significance level of Mann–Whitney U test. ADC, apparent diffusion coefficient; GS, Gleason score.

Frac < 1.0 were significantly higher and ADC values were significantly lower in GS ≥ 4 + 3 cancers than in GS ≤ 3 + 4 cancers (P < 0.01, P < 0.01, P < 0.01, P = 0.01, and P < 0.01, respectively). Frac > 3.0 was not significantly different between GS ≥ 4 + 3 cancers and GS ≤ 3 + 4 cancers (P = 0.59). In addition, Frac < 0.3, Frac < 0.5, and Frac < 0.8 were significantly higher, and ADC values were significantly lower in GS ≥ 3 + 4 cancers than in GS = 3 + 3 cancers (P < 0.01, P < 0.01, P = 0.04, and 0.03, respectively). Frac < 1.0 and Frac > 3.0 were not significantly different between GS ≥ 3 + 4 cancers and GS = 3 + 3 cancers (P = 0.07 and 0.46, respectively).

Table 3 and Fig. 2 show the diagnostic performance of Frac < 0.3, Frac < 0.5, Frac < 0.8, and ADC values. For discriminating GS ≥ 4 + 3 cancers from GS ≤ 3 + 4 cancers, the AUC for the ROC analysis ranged from 0.64 to 0.73, and significant differences in AUC were observed between Frac < 0.3 mm^2/s and ADC (P = 0.03), Frac < 0.5 mm^2/s and ADC (P < 0.01), Frac < 0.3 and Frac < 0.8 (P = 0.04), and Frac < 0.5 and Frac < 0.8 (P < 0.01). Frac < 0.3 mm^2/s and Frac < 0.5 mm^2/s had significantly greater AUC for discriminating GS ≥ 4 + 3 cancers from GS ≤ 3 + 4 cancers than ADC. On the other hand, Frac < 1.0 mm^2/s had significantly smaller AUC for discriminating GS ≥ 4 + 3 cancers from GS ≤ 3 + 4 cancers than ADC (P = 0.02). There were no significant differences between Frac < 0.3 and Frac < 0.5 (P = 0.32), and Frac < 0.8 and ADC (P = 0.81). For discriminating GS ≥ 3 + 4 cancers and GS = 3 + 3 cancers, the AUC ranged from 0.65 to 0.74, and there were no significant differences among these values (P = 0.10–0.49) (Table 4 and Fig. 3).

The correlation coefficients between the parameters and the Gleason scores (GS = 3 + 3, GS = 3 + 4, GS = 4 + 3) are 0.4 for Frac < 0.3, 0.36 for Frac < 0.5, 0.26 for Frac < 0.8, 0.21 for Frac < 1.0, −0.05 for Frac > 3.0, and −0.26 for ADC, respectively (P < 0.01, each).

Discussion

In this study, we found that the parameters obtained from the gamma model (Frac < 0.3, Frac < 0.5, Frac < 0.8) as well as ADC values showed significant differences between GS ≥ 4 + 3 and GS ≤ 3 + 4 cancers and between GS ≥ 3 + 4 and GS = 3 + 3 cancers. In addition, Frac < 0.3 and Frac < 0.5 showed higher diagnostic performance than ADC values for differentiating GS ≥ 4 + 3 and GS ≤ 3 + 4 cancers, although Frac < 0.3, Frac < 0.5, and ADC values showed similar diagnostic performance for differentiating GS ≥ 3 + 4 and GS = 3 + 3 cancers. Previous studies have demonstrated an inverse correlation between GS and ADC values.[14–17] However, there is a considerable overlap in ADC values between cancers of various grades.[8] In addition, although ADC values are based on free diffusion, diffusion is restricted by the presence of various barriers in biologic tissues. Thus, a new diffusion metric that may allow for improved discrimination between various grades of prostate cancer is desirable. Our study suggests that the parameters obtained from the gamma model may provide additional information for discriminating GS ≥ 4 + 3 from GS ≤ 3 + 4 prostate cancers.

This study demonstrated that Frac < 0.3 and Frac < 0.5 significantly outperformed ADC values for differentiation of GS ≥ 4 + 3 and GS ≤ 3 + 4 cancers, and were similar to ADC values

Table 3 The diagnostic performance of Frac < 0.3, Frac < 0.5, Frac < 0.8, Frac < 1.0, Frac > 3.0 and ADC for discriminating Gleason score (GS) ≥ 4 + 3 cancers from GS ≤ 3 + 4 cancers

Parameter	AUC	Sensitivity	Specificity	Cut-off value
Frac < 0.3 (%)	0.73	77.9	60.9	>15.9
	$P = 0.03^{*}$			
Frac < 0.5 (%)	0.71	82.1	53.1	>27.4
	$P < 0.01^{*}$			
Frac < 0.8 (%)	0.64	84.2	45.3	>41.6
	$P = 0.81$			
Frac < 1.0 (%)	0.62	83.2	40.6	>49.6
	$P = 0.02^{**}$			
Frac > 3.0 (%)	0.53	80	32.8	<12.68
	$P = 0.01^{**}$			
ADC (mm^2/s)	0.65	87.4	37.5	<0.87
	—			

*The parameter had a greater AUC than ADC; **The parameter had a smaller AUC than ADC; Statistical analyses were performed using the DeLong test was used to compare measures in terms of area under the receiver operating characteristic (ROC) curve AUC, *P*-values indicate the significance level of the DeLong test comparing AUC between each parameter obtained from the gamma model and ADC. ADC, apparent diffusion coefficient; AUC, area under the ROC curve.

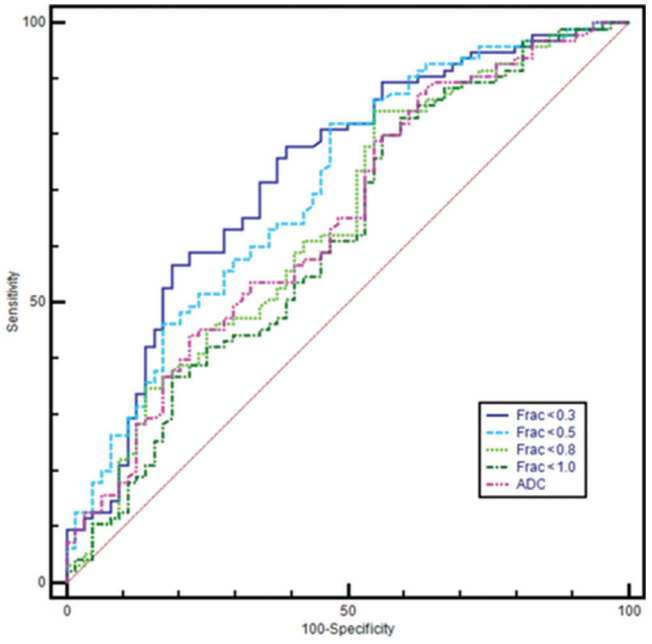

Fig. 2 Graph shows receiver operating characteristic (ROC) curves for detection of Gleason score (GS) ≥ 3 + 4 and GS ≥ 4 + 3 prostate cancer using the gamma model and ADC, area under the ROC curve ranged from 0.62 to 0.73, and significant differences were observed between Frac < 0.3 and ADC, Frac < 0.5 and ADC, Frac < 0.3 and Frac < 0.8, and Frac < 0.5 and Frac < 0.8 ($P = 0.03$, $P < 0.01$, $P = 0.04$, $P < 0.01$, respectively). ADC, apparent diffusion coefficient.

in differentiating GS ≥ 3 + 4 and GS = 3 + 3 cancers. As mentioned above, Epstein et al. found large differences in recurrence rates between GS ≥ 4 + 3 and GS ≤ 3 + 4 cancers. Thus, discriminating GS ≥ 4 + 3 from GS ≤ 3 + 4 prostate cancers on the basis of diffusion metrics might be of clinical importance.[10] Although ADC values were also significantly different between GS ≥ 4 + 3 and GS ≤ 3 + 4 cancers, the gamma model may provide more precise information for differentiating GS ≥ 4 + 3 and GS ≤ 3 + 4 cancers in our findings.

As stated above, Frac < 0.3 and Frac < 0.5 showed higher diagnostic performance than ADC for differentiating GS ≥ 4 + 3 from GS ≤ 3 + 4 cancers in this study. In the previous reports, Frac < 1.0 was an effective parameter for distinguishing healthy prostate glandular components from prostate cancer and was considered to be associated with restricted diffusion.[11,12] In this context, Frac < 0.3 and Frac < 0.5 would be associated with heavily restricted diffusion. As many papers have shown statistically significant correlations between the ADC values and the GS of prostate cancer. It would be rational for Frac < 0.3 and Frac < 0.5 to correlate more strongly with a higher GS than Frac < 1.0.

The gamma model is one of the non-monoexponential approaches for characterizing diffusion behavior in biological tissue. There are other approaches to describe the non-monoexponential diffusion behavior in the prostate gland, such as the stretched-exponential model,[18] intravoxel incoherent motion model,[19,20] and diffusion kurtosis imaging (DKI) findings.[21–23] Recently, Tamada et al.[23] reported that kurtosis (*K*), which is a parameter of DKI, provided no clear diagnostic benefit over ADC. However, although *K* is thought to be an index of microstructural complexity, the physiologic basis of *K* remains uncertain. In contrast, Frac < 0.3 and Frac < 0.5 reflect heavily restricted diffusion probably owing to a higher cellularity. Our preliminary findings suggest that

Table 4 The diagnostic performance of Frac < 0.3, Frac < 0.5, Frac < 0.8, Frac < 1.0, Frac > 3.0 and ADC values for discriminating Gleason score (GS) ≥ 3 + 4 cancers from GS ≤ 3 + 3 cancers

Parameter	AUC	Sensitivity	Specificity	Cut-off value
Frac < 0.3 (%)	0.74	60.3	84.6	>17.3
	$P = 0.49$			
Frac < 0.5 (%)	0.72	73.3	76.9	>27.1
	$P = 0.32$			
Frac < 0.8 (%)	0.67	76	69.2	>41.6
	$P = 0.45$			
Frac < 1.0 (%)	0.65	67.1	69.2	>52.6
	$P = 0.10$			
Frac > 3.0 (%)	0.56	63	61.5	<9.53
	$P = 0.05$			
ADC (mm^2/s)	0.69	72.6	69.2	<0.83
	—			

Statistical analyses were performed using the DeLong test was used to compare measures in terms of area under the receiver operating characteristic (ROC) curve AUC; *P*-values indicate the significance level of the DeLong test comparing AUC between each parameter obtained from the gamma model and ADC. ADC, apparent diffusion coefficient; AUC, area under the ROC curve.

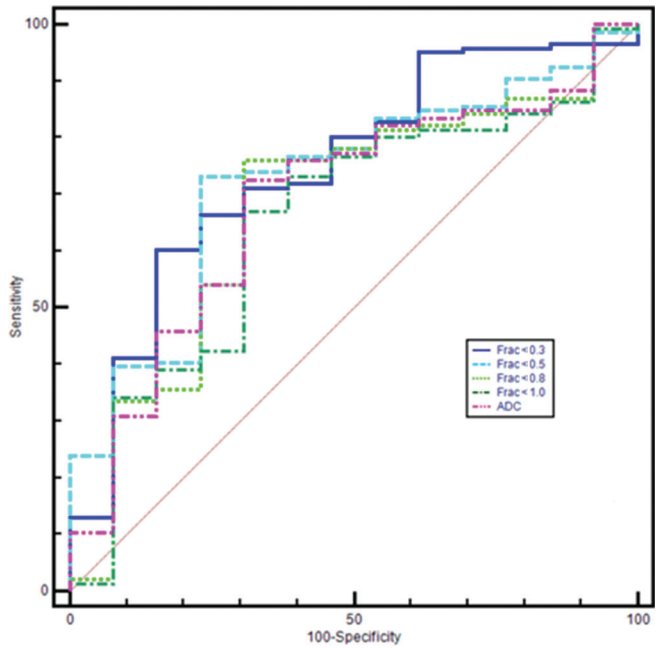

Fig. 3 Graph shows receiver operating characteristic (ROC) curves for detection of Gleason score (GS) ≥ 3 + 4 and GS = 3 + 3 prostate cancer with the gamma model and apparent diffusion coefficient. The area under the ROC curve ranged from 0.65 to 0.74, and there were no significant differences among these values ($P = 0.10$–0.49) ADC, apparent diffusion coefficient.

Frac < 0.3 and Frac < 0.5 may add additional value in discrimination of tumor grades.

Recently, Ahmed et al.[24] reported that using MP-MRI to triage men would avoid unnecessary biopsies in one-quarter of patients, and this strategy could improve the detection of clinically important prostate cancer and thereby reduce the number of men diagnosed with clinically insignificant cancer. In addition, according to PI-RADS version 2, the score obtained from DWI and the ADC map is the dominant parameter for determining the overall PI-RADS score for clinically significant cancer in the peripheral zone.[25] Thus, increasing ability of DWI to differentiate clinically significant cancer from clinically insignificant cancer using a new diffusion metric is a matter of clinical importance.

Our study has several limitations. First, our case selection may have been affected by bias because this was a retrospective study conducted at a single facility. The use of consensus readings must also be noted as a study limitation. Second, only 28 patients underwent radical prostatectomy, whereas the remaining 127 patients were diagnosed by systematic TRUS-guided 12-core biopsies with 2–4 additional targeted biopsies. Because MP-MRI findings do not correspond directly to the results of systematic biopsy, there was difficulty in ensuring the correspondence of biopsy sites to the suspicious area of prostate cancer on MP-MRI. In patients with prostate cancer who had undergone needle biopsy, 36.3% of those with a history of radical prostatectomy reported an upgrading of the GS,[26] which may also be related to the results. This may be the reasons why the AUC of the ADC and the correlation coefficients between the parameters of this study and the Gleason scores were lower than those of previous reports.[3,5,17,23] Third, this study was performed using two different MR scanners (3T and 1.5T). It would be better to conduct a study using an identical scanner, even though the diffusion signal decay does not depend on the field strength.[27,28] Finally, in this study, no significant difference was observed between Frac < 0.3 and Frac < 0.5. Further investigation to identify the parameter that is most suitable for the discrimination of tumor grades is needed.

Conclusion

In conclusion, we demonstrated that Frac < 0.3 and Frac < 0.5, which are parameters obtained from the gamma model, were significantly higher in GS ≥ 4 + 3 than in GS ≤ 3 + 4 cancers, and in GS ≥ 3 + 4 than in GS = 3 + 3 cancers. In addition, Frac < 0.3 and Frac < 0.5 showed higher diagnostic performance than ADC values for differentiating GS ≥ 4 + 3 from GS ≤ 3 + 4 cancers. The gamma model may add additional value in discrimination of tumor grades.

Conflicts of Interest

The authors declare that they have no conflicts of interest.

References

1. Bray F, Ferlay J, Soerjomataram I, Siegel RL, Torre LA, Jemal A. Global cancer statistics 2018: GLOBOCAN estimates of incidence and mortality worldwide for 36 cancers in 185 countries. CA Cancer J Clin 2018; 68:394–424.
2. El-Shater Bosaily A, Parker C, Brown LC, et al. PROMIS—Prostate MR imaging study: a paired validating cohort study evaluating the role of multi-parametric MRI in men with clinical suspicion of prostate cancer. Contemp Clin Trials 2015; 42:26–40.
3. Hambrock T, Somford DM, Huisman HJ, et al. Relationship between apparent diffusion coefficients at 3.0-T MR imaging and Gleason grade in peripheral zone prostate cancer. Radiology 2011; 259:453–461.
4. Tanimoto A, Nakashima J, Kohno H, Shinmoto H, Kuribayashi S. Prostate cancer screening: the clinical value of diffusion-weighted imaging and dynamic MR imaging in combination with T2-weighted imaging. J Magn Reson Imaging 2007; 25:146–152.
5. Oto A, Kayhan A, Jiang Y, et al. Prostate cancer: differentiation of central gland cancer from benign prostatic hyperplasia by using diffusion-weighted and dynamic contrast-enhanced MR imaging. Radiology 2010; 257:715–723.
6. Moldovan PC, Van den Broeck T, Sylvester R, et al. What is the negative predictive value of multiparametric magnetic resonance imaging in excluding prostate cancer at biopsy? A systematic review and meta-analysis from the european association of urology prostate cancer guidelines panel. Eur Urol 2017; 72:250–266.
7. Weinreb JC, Barentsz JO, Choyke PL, et al. PI-RADS Prostate Imaging - Reporting and Data System: 2015, Version 2. Eur Urol 2016; 69:16–40.
8. Wibmer AG, Sala E, Hricak H, Vargas HA. The expanding landscape of diffusion-weighted MRI in prostate cancer. Abdom Radiol (NY) 2016; 41:854–861.
9. Epstein JI, Zelefsky MJ, Sjoberg DD, et al. A contemporary prostate cancer grading system: a validated alternative to the Gleason Score. Eur Urol 2016; 69:428–435.
10. Epstein JI, Egevad L, Amin MB, Delahunt B, Srigley JR, Humphrey PA; Grading Committee. The 2014 International Society of Urological Pathology (ISUP) consensus conference on gleason grading of prostatic carcinoma: definition of grading patterns and proposal for a new grading system. Am J Surg Pathol 2016; 40:244–252.
11. Oshio K, Shinmoto H, Mulkern RV. Interpretation of diffusion MR imaging data using a gamma distribution model. Magn Reson Med Sci 2014; 13:191–195.
12. Shinmoto H, Oshio K, Tamura C, et al. Diffusion-weighted imaging of prostate cancer using a statistical model based on the gamma distribution. J Magn Reson Imaging 2015; 42:56–62.
13. Epstein JI. An update of the Gleason grading system. J Urol 2010; 183:433–440.
14. Sato C, Naganawa S, Nakamura T, et al. Differentiation of non-cancerous tissue and cancer lesions by apparent diffusion coefficient values in transition and peripheral zones of the prostate. J Magn Reson Imaging 2005; 21:258–262.
15. Tamada T, Sone T, Jo Y, et al. Apparent diffusion coefficient values in peripheral and transition zones of the prostate: comparison between normal and malignant prostatic tissues and correlation with histologic grade. J Magn Reson Imaging 2008; 28:720–726.
16. Itou Y, Nakanishi K, Narumi Y, Nishizawa Y, Tsukuma H. Clinical utility of apparent diffusion coefficient (ADC) values in patients with prostate cancer: can ADC values contribute to assess the aggressiveness of prostate cancer? J Magn Reson Imaging 2011; 33:167–172.
17. Verma S, Rajesh A, Morales H, et al. Assessment of aggressiveness of prostate cancer: correlation of apparent diffusion coefficient with histologic grade after radical prostatectomy. AJR Am J Roentgenol 2011; 196:374–381.
18. Bennett KM, Schmainda KM, Bennett RT, Rowe DB, Lu H, Hyde JS. Characterization of continuously distributed cortical water diffusion rates with a stretched-exponential model. Magn Reson Med 2003; 50:727–734.
19. Döpfert J, Lemke A, Weidner A, Schad LR. Investigation of prostate cancer using diffusion-weighted intravoxel incoherent motion imaging. Magn Reson Imaging 2011; 29:1053–1058.
20. Shinmoto H, Tamura C, Soga S, et al. An intravoxel incoherent motion diffusion-weighted imaging study of prostate cancer. AJR Am J Roentgenol 2012; 199:W496–W500.
21. Rosenkrantz AB, Sigmund EE, Johnson G, et al. Prostate cancer: feasibility and preliminary experience of a diffusional kurtosis model for detection and assessment of aggressiveness of peripheral zone cancer. Radiology 2012; 264:126–135.
22. Tamura C, Shinmoto H, Soga S, et al. Diffusion kurtosis imaging study of prostate cancer: preliminary findings. J Magn Reson Imaging 2014; 40:723–729.
23. Tamada T, Prabhu V, Li J, Babb JS, Taneja SS, Rosenkrantz AB. Prostate cancer: diffusion-weighted MR imaging for detection and assessment of aggressiveness-comparison between conventional and kurtosis models. Radiology 2017; 284:100–108.
24. Ahmed HU, El-Shater Bosaily A, Brown LC, et al. Diagnostic accuracy of multi-parametric MRI and TRUS biopsy in prostate cancer (PROMIS): a paired validating confirmatory study. Lancet 2017; 389:815–822.

25. Purysko AS, Rosenkrantz AB, Barentsz JO, Weinreb JC, Macura KJ. PI-RADS Version 2: a pictorial update. Radiographics 2016; 36:1354–1372.
26. Epstein JI, Feng Z, Trock BJ, Pierorazio PM. Upgrading and downgrading of prostate cancer from biopsy to radical prostatectomy: incidence and predictive factors using the modified Gleason grading system and factoring in tertiary grades. Eur Urol 2012; 61:1019–1024.
27. Ogura A, Tamura T, Ozaki M, et al. Apparent diffusion coefficient value is not dependent on magnetic resonance systems and field strength under fixed imaging parameters in brain. J Comput Assist Tomogr 2015; 39:760–765.
28. Donati OF, Chong D, Nanz D, et al. Diffusion-weighted MR imaging of upper abdominal organs: field strength and intervendor variability of apparent diffusion coefficients. Radiology 2014; 270:454–463.